Published in final edited form as:
Mol Microbiol. 2014 June ; 92(6): 1212–1226. doi:10.1111/mmi.12623.

A role for FtsA in SPOR-independent localization of the essential *Escherichia coli* cell division protein FtsN

Kimberly K. Busiek and **William Margolin***
Department of Microbiology and Molecular Genetics, University of Texas Medical School at Houston, Houston, Texas, USA

SUMMARY

FtsN is a bitopic membrane protein and the last essential component to localize to the *Escherichia coli* cell division machinery, or divisome. The periplasmic SPOR domain of FtsN was previously shown to localize to the divisome in a self-enhancing manner, relying on the essential activity of FtsN and the peptidoglycan synthesis and degradation activities of FtsI and amidases, respectively. Because FtsN has a known or purported role in stimulation of these activities, it follows that FtsN initially localizes to division sites in a SPOR-independent manner. Here, we show that the cytoplasmic and transmembrane domains of FtsN ($FtsN_{Cyto\text{-}TM}$) facilitated localization of FtsN independently of its SPOR domain but dependent on the early cell division protein FtsA. In addition, SPOR-independent localization preceded SPOR-dependent localization, providing a mechanism for the initial localization of FtsN. In support of the role of $FtsN_{Cyto\text{-}TM}$ in FtsN function, a variant of FtsN lacking the cytoplasmic domain localized to the divisome but failed to complement an *ftsN* deletion unless it was overproduced. Simultaneous removal of both domains abolished localization and complementation. These data support a model in which FtsA-FtsN interaction recruits FtsN to the divisome, where it can then stimulate the peptidoglycan remodeling activities required for SPOR-dependent localization.

Keywords

cell division; cytokinesis; FtsA

INTRODUCTION

Division of a single cell into two equal daughter cells is a fundamental process shared among eukaryotic and prokaryotic organisms. Yet, despite the conservation of this developmental stage, we continue to lack a complete understanding of the mechanisms driving cytokinesis. To further characterize this process, the essential proteins and protein-protein interactions that participate in cell division must be further investigated. At present, nearly a dozen essential cell division proteins have been identified in the model bacterium *Escherichia coli* (Rico et al., 2013). These proteins comprise a division machine or "divisome" that assembles at midcell into a ring-shaped structure prior to cytokinesis.

*Corresponding author. Mailing address: Department of Microbiology and Molecular Genetics, University of Texas Medical School at Houston, 6410 Fannin Street, Houston, TX 77030. Phone: (713) 500-5452. William.Margolin@uth.tmc.edu.

The components of the *E. coli* divisome are incorporated in two overall stages, with some proteins localizing early to midcell and others localizing late (Aarsman *et al.*, 2005). FtsZ, a homolog of eukaryotic tubulin, is the first essential cell division protein to localize at midcell (Erickson, 1997). FtsZ marks the division site by polymerizing into a ring structure (Z-ring) that serves as a scaffold for the remaining cell division proteins (Bi and Lutkenhaus, 1991). FtsA and ZipA are recruited to the division site soon after polymerization of FtsZ and tether the Z-ring to the inner membrane (Ma *et al.*, 1996, Raychaudhuri, 1999, Pichoff and Lutkenhaus, 2002, Pichoff and Lutkenhaus, 2005). Once the early divisome proteins are assembled at midcell, the late cell division proteins are recruited at a defined later stage (Aarsman et al., 2005) in a linear order of dependency (FtsK → FtsQBL complex → FtsW → FtsI → FtsN). The order of essential cell division protein recruitment is based on several pioneering studies in which one or more divisome proteins were inactivated and the localization of downstream cell division proteins was monitored [reviewed in (Goehring and Beckwith, 2005) and (Vicente and Rico, 2006)].

Despite the established order of dependency, recent studies have suggested that recruitment of many cell division proteins is more complicated. FtsN, for example, fails to localize to division sites in the absence of FtsA even after all other essential cell division proteins, including FtsI, are artificially targeted to midcell (Goehring *et al.*, 2005). FtsN is a transmembrane protein with a small cytoplasmic tail, a single transmembrane segment, and a relatively large periplasmic domain (Dai *et al.*, 1993). Because FtsN is an essential cell division protein, FtsN depletion causes cell filamentation and eventual death (Dai et al., 1993). Although the essential function of FtsN is unknown, FtsN appears to have a role in divisome stabilization, as removal of FtsN leads to disassembly of divisome components (Rico *et al.*, 2010). Domain swap experiments showed that the cytoplasmic and transmembrane domains of FtsN can be replaced by analogous domains from other proteins and still complement an *ftsN* null mutant (Dai *et al.*, 1996, Addinall *et al.*, 1997, Goehring *et al.*, 2007, Gerding *et al.*, 2009). The domain of FtsN essential for its function was pinpointed to a three-alpha helix segment in the membrane-proximal region of the periplasmic domain. In addition, the C-terminal region of FtsN harbors a SPOR domain involved in binding peptidoglycan (Ursinus *et al.*, 2004), which is also present in several other *E. coli* proteins (Gerding et al., 2009, Arends *et al.*, 2010).

FtsN localizes to the divisome most efficiently via its periplasmic SPOR domain. This localization requires three activities: the peptidoglycan synthesis activity of penicillin binding protein FtsI (PBP3); the essential activity of FtsN, as accomplished by FtsN itself or by its suppressor, FtsA(E124A); and the activity of at least one periplasmic murein amidase (Gerding et al., 2009). Although SPOR-mediated localization of FtsN is dependent upon prior activation of these proteins, FtsN has a demonstrated role in the recruitment of amidases and an implied role in FtsI stimulation, suggesting that its targeting to the divisome is self-reinforced. Specifically, the recruitment of amidases AmiB and AmiC to division sites is dependent on FtsN, as is the localization of NlpD, the cognate activator of AmiC (Peters *et al.*, 2011). FtsN has also been shown to activate PBP1b and is suspected of activating FtsI (Muller *et al.*, 2007). If FtsN is involved in the initial localization and stimulation of these proteins, how does FtsN get to the divisome in the first place?

Here, we provide evidence that the previously established interaction between FtsA and FtsN (Karimova *et al.*, 2005, Corbin *et al.*, 2004, Busiek *et al.*, 2012) facilitates midcell localization of FtsN. We also show that this SPOR-independent means of FtsN localization precedes SPOR-dependent midcell recruitment. Together, these results provide a mechanism for the initial localization of FtsN that is needed for recruitment or stimulation of FtsI, FtsN, and amidase activities and subsequent SPOR-dependent localization of FtsN.

RESULTS

The cytoplasmic domain of FtsN contributes to its localization to the divisome independently of native FtsN

Previously, our laboratory provided *in vitro* evidence that proteins FtsA and FtsN interact, and that the first 55 residues of FtsN, including the short cytoplasmic tail and transmembrane domain ($FtsN_{Cyto\text{-}TM}$) are sufficient for this interaction (Busiek et al., 2012). We also found that strong overproduction of $FtsN_{Cyto\text{-}TM}$ caused moderate filamentation of cells (data not shown), which prompted us to ask if the cytoplasmic and transmembrane domains of FtsN can localize to division sites without the aid of the known divisome targeting determinants in the periplasmic domain. To observe the localization of $FtsN_{Cyto\text{-}TM}$, we fused green fluorescent protein (GFP) to the amino terminus of $FtsN_{Cyto\text{-}TM}$ (Fig. 1A) and expressed the fusion at uninduced levels from plasmid pDSW207, which has a weakened *trc* promoter with leaky expression. Although GFP itself localized diffusely throughout the cell (Fig. 1B), GFP-$FtsN_{Cyto\text{-}TM}$ localized specifically to division sites and the membrane (Fig. 1C). The ability of FtsN to localize weakly in the absence of the SPOR domain was also noted when observing GFP fusions to $FtsN_{1–243}$, $FtsN_{1–105}$, and $FtsN_{1–90}$ (Gerding et al., 2009).

To narrow down the segment of $FtsN_{Cyto\text{-}TM}$ required for midcell localization, we replaced the cytoplasmic and transmembrane segments of $FtsN_{Cyto\text{-}TM}$ with the corresponding domains of the unrelated *Agrobacterium tumefaciens* protein VirB10. VirB10 is a key component of the Type IV secretion system and has a bitopic membrane topology similar to FtsN (Garza and Christie, 2013). GFP-$VirB10_{Cyto}N_{TM}$ localized uniformly around the membrane but failed to localize to division sites (Fig. 1D), whereas GFP-$FtsN_{Cyto}VirB10_{TM}$ localized clearly to midcell (Fig. 1E). These results indicate that the FtsN cytoplasmic domain is sufficient to promote midcell localization of GFP-$FtsN_{Cyto\text{-}TM}$. However, GFP-$FtsN_{Cyto}$ alone did not localize to division sites (data not shown), suggesting that the transmembrane domain of VirB10 facilitates midcell localization of GFP-$FtsN_{Cyto}VirB10_{TM}$, possibly through the weak dimeric activity or membrane association of $VirB10_{TM}$ (Garza and Christie, 2013). Consistent with this idea, the cytoplasmic domain of FtsN alone fails to interact with FtsA unless it is fused to a dimerization motif, such as a leucine zipper (Busiek et al., 2012).

Because self-interaction of FtsN was previously reported (Karimova et al., 2005, Alexeeva *et al.*, 2010), we wanted to rule out the possibility that GFP-$FtsN_{Cyto\text{-}TM}$ localizes to division sites through its interaction with native FtsN. If midcell localization of GFP-$FtsN_{Cyto\text{-}TM}$ is indeed dependent on interaction with previously localized FtsN, then loss of FtsN should result in delocalization of GFP-$FtsN_{Cyto\text{-}TM}$. Although FtsN is an essential cell

division protein, cells can survive the loss of *ftsN* when a single amino acid mutation in FtsA (FtsA-E124A) is present (Bernard *et al.*, 2007). Using an *ftsN* deletion strain carrying a chromosomal *ftsA-E124A* allele (WM3302), we observed localization of GFP-FtsN$_{Cyto-TM}$ at division sites in 87% of cells, indicating that GFP-FtsN$_{Cyto-TM}$ is efficiently recruited to the divisome independently of FtsN (Fig. 1F).

Localization of GFP-FtsN$_{Cyto-TM}$ to midcell is dependent on FtsA

Because the amino terminus of FtsN interacts with cell division protein FtsA, we hypothesized that FtsA recruits GFP-FtsN$_{Cyto-TM}$ directly to division sites. Using the *ftsA12*(Ts) strain WM1115, we compared the localization of GFP-FtsN$_{Cyto-TM}$ at the permissive temperature of 30°C to the pattern of localization at the non-permissive temperature of 42°C. Because FtsA12 delocalizes from division sites within 5 minutes at 42°C (Fig. S1), we visualized cells 5 minutes after the temperature shift. GFP-FtsN$_{Cyto-TM}$ formed midcell rings at the permissive temperature as expected, but delocalized within the 5 minute temperature shift (Fig. 2). Similar results were seen when we monitored the localization of GFP-tagged FtsN$_{\Delta SPOR}$, a construct that retains the cytoplasmic and transmembrane domains of FtsN but lacks the SPOR domain (Fig. 1A and data not shown). It is unlikely that thermal instability or other non-specific factors caused GFP-FtsN$_{Cyto-TM}$ to delocalize, as GFP-FtsN$_{Cyto-TM}$ continued to form fluorescent rings at midcell after 5 or 30 minutes at 42°C in WM1074, the wild-type parent of WM1115 (Fig. S2).

Localization of FtsN's SPOR domain requires the peptidoglycan synthesis activity of FtsI (Gerding et al., 2009). To understand if localization of GFP-FtsN$_{Cyto-TM}$ has a similar requirement, we treated cells with cephalexin, an inhibitor of FtsI activity, and visualized cells for altered localization. As a negative control, we observed the localization of the isolated SPOR domain (FtsN$_{SPOR}$) after cephalexin treatment. Because the SPOR domain is periplasmic, we tagged FtsN$_{SPOR}$ with Tat-targeted mCherry (^{TT}mCherry-FtsN$_{SPOR}$). ^{TT}mCherry harbors the signal sequence of TorA, a Tat-targeted substrate that allows efficient export of FtsN$_{SPOR}$ to the periplasm (Thomas *et al.*, 2001). As expected, ^{TT}mCherry-FtsN$_{SPOR}$ delocalized within 30 minutes of cephalexin treatment, confirming that SPOR-dependent localization of FtsN requires the peptidoglycan synthesis activity of FtsI. Unlike ^{TT}mCherry-FtsN$_{SPOR}$, GFP-FtsN and GFP-FtsN$_{Cyto-TM}$ continued to localize after cephalexin treatment, demonstrating that the cytoplasmic and transmembrane domains of FtsN have different requirements for localization than the SPOR domain (Fig. 3). Although rapid cell lysis has been described during cephalexin treatment of *E. coli* cells under specific conditions (Chung *et al.*, 2009), we did not observe lysis using our standard growth conditions. Additionally, we tested whether FtsQ or FtsI are needed for localization of GFP-FtsN$_{Cyto-TM}$. Both FtsQ and FtsI interacted with FtsN in previously published *in vivo* studies, and could potentially recruit GFP-FtsN$_{Cyto-TM}$ to midcell (Karimova et al., 2005). However, GFP-FtsN$_{Cyto-TM}$ continued to localize at potential division sites after thermoinactivation of *ftsQ*(Ts) or *ftsI*(Ts) at 42°C (Fig. S3 and Table S2), suggesting that neither FtsQ nor FtsI promotes SPOR-independent localization of FtsN.

We then asked whether full length FtsN depended on FtsA for its localization. Like GFP-FtsN$_{Cyto-TM}$, GFP-FtsN localized at the permissive temperature in the *ftsA12*(Ts) strain (Fig.

2). Localization of GFP-FtsN at midcell decreased in frequency after thermoinactivation at 42°C (Table 2), but weak fluorescent rings could still be observed at division sites at 42°C, perhaps via SPOR-dependent localization. To test this hypothesis, we observed the localization of ^{TT}mCherry-FtsN$_{SPOR}$ in the *ftsA12*(Ts) strain at the non-permissive temperature. ^{TT}mCherry-FtsN$_{SPOR}$ remained at midcell after thermoinactivation of *ftsA12*(Ts) (Fig. 2), supporting the idea that the SPOR domain of FtsN localizes to the divisome independently of FtsA. Not surprisingly, GFP-tagged FtsZ, which does not depend solely on FtsA for localization (Pichoff and Lutkenhaus, 2002), remained largely unaffected by the temperature shift, forming fluorescent rings at 42°C. Overall, the failure of GFP-FtsN$_{Cyto-TM}$ to form fluorescent rings in the *ftsA12*(Ts) strain at the non-permissive temperature suggests that localization of GFP-FtsN$_{Cyto-TM}$ to division sites is dependent on proper localization of FtsA.

To test whether FtsA is sufficient to recruit FtsN$_{Cyto-TM}$, we turned to our polar recruitment assay, which previously showed for the first time that FtsA and full-length FtsN could interact (Corbin et al., 2004). Briefly, a bait protein is fused to the *Bacillus subtilis* protein DivIVA that preferentially localizes to areas of curvature within any cell, which in *E. coli* are the cell poles and division septa (Edwards *et al.*, 2000). If the co-produced GFP-tagged prey protein is a divisome protein and interacts with the bait protein, the prey will relocalize from solely the septum to the cell poles as well as the septum. This change in fluorescence localization is an easy visual readout (Ding *et al.*, 2002). For the current experiment, bait protein FtsA was fused to DivIVA (pBAD33-*divIVA-ftsA*) and prey protein FtsN$_{Cyto-TM}$ was fused to GFP (pDSW207-*gfp-ftsN$_{Cyto-TM}$*). Upon induction of *gfp-ftsN$_{Cyto-TM}$* expression only, GFP-FtsN$_{Cyto-TM}$ localized to cell division sites but did not accumulate at poles (Fig. 4A, top middle panel). When expression of both *gfp-ftsN$_{Cyto-TM}$* and *divIVA-ftsA* was induced, however, GFP-FtsN$_{Cyto-TM}$ localized not only at division sites, but also the cell poles, indicating that DivIVA-FtsA can efficiently recruit GFP-FtsN$_{Cyto-TM}$ to cell poles (Fig. 4A, bottom middle panel, arrow). Additionally, we confirmed that DivIVA-FtsA does not affect the diffuse localization of unfused GFP but does recruit GFP-FtsN to cell poles as reported in Corbin *et al.* (2004) (Fig. 4A, left and right panels, arrow).

Because GFP-FtsN$_{Cyto-TM}$ localized to midcell in a Δ*ftsN ftsA-E124A* strain that lacks the wild-type *ftsA* allele (Fig. 1F), we asked whether the FtsA with the E124A lesion can interact with FtsN by investigating whether DivIVA-FtsA-E124A could recruit GFP-FtsN$_{Cyto-TM}$ to cell poles. Like DivIVA-FtsA, DivIVA-FtsA-E124A recruited both GFP-FtsN$_{Cyto-TM}$ and GFP-FtsN to sites of cell curvature (Fig. 4B, arrows). Based on the delocalization of GFP-FtsN$_{Cyto-TM}$ upon thermoinactivation of FtsA12(Ts) (Fig. 2) and the polar recruitment of GFP-FtsN$_{Cyto-TM}$ by DivIVA-FtsA and DivIVA-FtsA-E124A (Fig. 4), we conclude that FtsA is likely necessary and sufficient for recruitment of GFP-FtsN$_{Cyto-TM}$ to division sites.

The cytoplasmic and SPOR domains of FtsN share overlapping roles in localization of FtsN

Although the FtsA-FtsN$_{Cyto-TM}$ interaction is capable of recruiting FtsN$_{Cyto-TM}$ to specific cellular locations, the periplasmic SPOR domain is thought to be the major localization

determinant of FtsN (Gerding et al., 2009). To elucidate the relative contributions of the cytoplasmic and SPOR domains to midcell localization of FtsN, we visualized cells producing GFP fusions to FtsN variants that lacked the native cytoplasmic domain ($VirB10_{Cyto}N_{TM\text{-}Peri}$), the SPOR domain ($FtsN_{\Delta SPOR}$), or both domains ($VirB10_{Cyto}N_{TM\text{-}Peri\Delta SPOR}$) and quantified the occurrence of midcell localization at non-constricting and constricting sites. We had also attempted to truncate the first 20 residues of the cytoplasmic domain of FtsN ($FtsN_{\Delta 1–20}$), but the construct was unstable (data not shown). Additionally, we mutated residues 16–19 that are involved in FtsA-FtsN interaction *in vitro* (Busiek et al., 2012) but, like $FtsN_{\Delta 1–20}$, this protein was also unstable (data not shown). Although GFP-$VirB10_{Cyto}N_{TM\text{-}Peri}$ and GFP-$FtsN_{\Delta SPOR}$ localized to potential division sites, the fusion lacking both domains (GFP-$VirB10_{Cyto}N_{TM\text{-}Peri\Delta SPOR}$) failed to localize (Fig. 5).

These results indicate that localization of FtsN requires either the cytoplasmic or SPOR domain for localization to potential division sites and that loss of both domains prevents recruitment of FtsN. Furthermore, the majority of fluorescent GFP-$VirB10_{Cyto}N_{TM\text{-}Peri}$ rings were located at division sites that were visibly constricting (64%), whereas the majority of fluorescent GFP-$FtsN_{\Delta SPOR}$ rings were located at non-constricting sites (62%; Table 3). These results imply that on average, GFP-$VirB10_{Cyto}N_{TM\text{-}Peri}$ localizes to midcell during a later stage of cytokinesis than GFP-$FtsN_{\Delta SPOR}$.

GFP-$FtsN_{Cyto\text{-}TM}$ localizes to midcell prior to ^{TT}mCherry-$FtsN_{SPOR}$

To test directly the hypothesis that SPOR-independent localization of FtsN precedes SPOR-dependent localization, we separately co-produced GFP-$FtsN_{Cyto\text{-}TM}$ and Tat-targeted mCherry (^{TT}mCherry) fused to $FtsN_{SPOR}$ in the same cell and compared their localization. The Tat-targeting sequence was fused to the mCherry-$FtsN_{SPOR}$ chimera to facilitate export of the construct to the periplasm (Thomas *et al.*, 2001). Although we observed frequent co-localization of GFP-$FtsN_{Cyto\text{-}TM}$ and ^{TT}mCherry-$FtsN_{SPOR}$ as expected, GFP-$FtsN_{Cyto\text{-}TM}$ and ^{TT}mCherry-$FtsN_{SPOR}$ also localized to division sites independent of one another. Specifically, rings of GFP-$FtsN_{Cyto\text{-}TM}$ were present at quarter sites of cells in the late stages of cytokinesis (denoted by arrows in Fig. 6), consistent with GFP-$FtsN_{Cyto\text{-}TM}$ localizing to nascent division sites. Conversely, ^{TT}mCherry-$FtsN_{SPOR}$ lingered at deep constrictions (denoted by asterisks in Fig. 6) and was often not detectable at the nascent division sites that contained GFP-$FtsN_{Cyto\text{-}TM}$ (arrows).

We quantified the difference in localization between the constructs by measuring the frequency of division site localization at constricting and non-constricting sites. In cells co-producing both fusions, the vast majority of GFP-$FtsN_{Cyto\text{-}TM}$ rings (83%) were located at non-constricting sites, whereas the majority of ^{TT}mCherry-$FtsN_{SPOR}$ rings were located at constrictions (62%; Table 4). We observed similar localization patterns when GFP-FtsN was co-produced with ^{TT}mCherry-$FtsN_{SPOR}$, although a larger proportion of GFP-FtsN rings were located at constricting sites. The higher percentage of GFP-FtsN rings at constricting sites compared to GFP-$FtsN_{Cyto\text{-}TM}$ is expected, as GFP-FtsN also contains the SPOR domain that, according to the above data, localizes preferentially to constricting sites.

Together, these data support the hypothesis that SPOR-independent localization of FtsN precedes SPOR-dependent localization.

Inactivation of cytoplasmic or SPOR domains inhibits the ability of FtsN to function in cell division

To explore the relative physiological importance of SPOR-independent and SPOR-dependent means of FtsN localization, we attempted to create strains carrying a single *ftsN* allele that lacked the cytoplasmic, SPOR, or both domains. To engineer these strains, we introduced the Δ*ftsN::kan* allele by P1 phage transduction into wild-type cells harboring plasmids pDSW210-*flag-virB10*$_{Cyto}$*N*$_{TM\text{-}Peri}$, -*ftsN*$_{\Delta SPOR}$, or -*virB10*$_{Cyto}$*N*$_{TM\text{-}Peri\Delta SPOR}$. Strains carrying pDSW210-*flag* or pDSW210-*flag-ftsN* were transduced as negative and positive controls, respectively. In the absence of inducer, leaky expression of *ftsN* from the weakened *trc* promoter of pDSW210 complemented the loss of the chromosomal *ftsN* allele (Fig. 7A, right column), whereas no transductants were found with empty pDSW210 vector at any IPTG concentration (Fig. 7A, left column). Induced expression of *flag-ftsN* also conferred survival in the absence of chromosomal *ftsN* at 10 μM and 100 μM IPTG, suggesting that higher levels of *ftsN* expression did not inhibit growth significantly as has been shown previously (Aarsman et al., 2005).

The various *ftsN* constructs were similarly tested for growth in the absence of chromosomal *ftsN*. None of the constructs could complement the loss of the native *ftsN* allele in the absence of inducer. However, in the presence of 10 μM IPTG, FLAG-FtsN$_{\Delta SPOR}$ partially complemented the loss of the native allele as evidenced by the small colonies formed on this plate. FLAG-FtsN$_{\Delta SPOR}$ completely complemented upon full induction of the plasmid (100 μM IPTG). Although FLAG-VirB10$_{Cyto}$N$_{TM\text{-}Peri}$ did not complement at 0 μM or 10 μM IPTG, full induction of *flag-virB10*$_{Cyto}$*N*$_{TM\text{-}Peri}$ conferred survival. FLAG-VirB10$_{Cyto}$N$_{TM\text{-}Peri\Delta SPOR}$ was unable to complement the loss of *ftsN* at any level of induction, consistent with the fluorescence microscopy results that showed no midcell localization of GFP-VirB10$_{Cyto}$N$_{TM\text{-}Peri\Delta SPOR}$(Fig. 5). The lack of complementation by FLAG-VirB10$_{Cyto}$N$_{TM\text{-}Peri\Delta SPOR}$ was not due to instability of the protein, because it was present at equal or greater levels than FLAG-FtsN$_{\Delta SPOR}$ or FLAG-FtsN, both of which were capable of complementing the loss of native FtsN (Fig. 7B). Importantly, anti-FtsN Western blot analysis showed that FLAG-FtsN was produced at a level equivalent to endogenous FtsN when induced at 10 μM IPTG (data not shown), indicating that each construct shown in Fig. 7B was produced at a level similar to native FtsN. Notably, a strain synthesizing FLAG-VirB10$_{Cyto}$N$_{TM\text{-}Peri}$ failed to survive the deletion of *ftsN* at levels of protein equivalent to or higher than FLAG-FtsN$_{\Delta SPOR}$ (Fig. 7A, 10 μM IPTG; compare protein levels at 10 and 100 μM IPTG in Fig. 7B), supporting the idea that SPOR-independent localization of FtsN plays an important role in proper localization of FtsN.

To confirm the transduction data, we also tested the effects of depleting FtsN in a strain carrying the same plasmids used in the transduction experiments. Consistent with our transduction data, FLAG-VirB10$_{Cyto}$N$_{TM\text{-}Peri\Delta SPOR}$ failed to complement the loss of *ftsN* at any level of induction and FLAG-FtsN$_{\Delta SPOR}$ began complementing at a lower level of induction than FLAG-VirB10$_{Cyto}$N$_{TM\text{-}Peri}$ (Fig. S4). Also consistent with the transduction

data, FLAG-FtsN complemented both in the absence and presence of inducer. Although substitution of the cytoplasmic and transmembrane regions or deletion of the SPOR domain did not result in cell death in previous publications (Dai et al., 1996, Addinall et al., 1997, Goehring et al., 2007, Gerding et al., 2009), all of these studies relied on overproduction of the mutated constructs. Our results are consistent with these previous results in that FLAG-VirB10$_{Cyto}$N$_{TM\text{-}Peri}$ and FLAG-FtsN$_{\Delta SPOR}$ could complement the loss of *ftsN*, but only when their expression was induced.

To ensure that the cell viability defects of the FtsN constructs were caused by inhibition of cell division and not a general problem with growth, we observed the morphology of the transduction survivors upon full IPTG induction of the plasmids and for several generations after depletion of inducer. As expected, Δ*ftsN::kan* cells producing FLAG-FtsN did not form filaments prior to or after depletion of IPTG (Fig. 7C, right panels). Transductants lacking chromosomal *ftsN* but producing FLAG-FtsN$_{\Delta SPOR}$, on the other hand, formed moderate filaments upon depletion of the inducer (Fig. 7C, middle panels), consistent with the results in Fig. 7A–B and Fig. S4. Also consistent with the transduction and spot dilution data, Δ*ftsN::kan* cells producing FLAG-VirB10$_{Cyto}$N$_{TM\text{-}Peri}$ were more affected by the lack of IPTG, forming long filaments, inferring that cell division was severely compromised. The impacts on cell division among the mutant FtsN strains at low levels of induction are compatible with the idea that these proteins localize poorly. These results suggest that although the cytoplasmic and SPOR domains have overlapping roles in localization, both domains are needed for efficient localization of FtsN to the divisome.

DISCUSSION

The data presented here support a model in which interaction between FtsA and FtsN weakly recruits FtsN to midcell by its amino-terminus following incorporation of FtsA into the divisome (Fig. 8). After its recruitment to the divisome, FtsN is poised to recruit amidases and stimulate the activity of FtsI. The activity of FtsN, amidases, and FtsI attracts additional FtsN molecules via the SPOR domain and reinforces a positive feedback loop. A similar model of self-enhanced recruitment of FtsN was first proposed by Gerding *et al.* (2009), but the mechanism of initial FtsN localization was unknown at the time.

SPOR-dependent localization of cell division proteins appears to be a common mechanism for division site recruitment: the SPOR domain of *E. coli* cell division proteins FtsN, DamX, DedD, and RlpA directs all four of these proteins to midcell (Gerding et al., 2009, Arends et al., 2010). Although SPOR-dependent localization of FtsN is supported by our data, we also highlight the need for the amino-terminus of FtsN in its recruitment to midcell. The requirement for both cytoplasmic and periplasmic domains for midcell localization has already been shown for the essential *E. coli* cell division protein FtsQ. Similar to FtsN, the cytoplasmic domain of FtsQ was originally described as a dispensable portion of the protein (Goehring et al., 2007). However, as with the experiments performed with FtsN proteins that lacked the cytoplasmic domain, these studies were performed at induced levels of the protein (Guzman *et al.*, 1997). It was later shown that the cytoplasmic domain of FtsQ is not dispensable and, in addition to its periplasmic localization determinant, it has a role in midcell localization of the protein (Goehring et al., 2007). The cytoplasmic and periplasmic

domains are not the only domains of the bitopic division proteins that contribute to localization. The localization of FtsI, for example, requires its transmembrane region (Wissel *et al.*, 2005). Although the transmembrane domain of FtsN is not directly involved in SPOR-independent localization (Fig. 1), our results suggest that putative dimerization of this domain (Busiek et al., 2012) is important for its interaction with FtsA and, hence, FtsA-dependent recruitment of FtsN.

The immediate delocalization of GFP-$FtsN_{Cyto\text{-}TM}$ from division sites upon shifting the *ftsA12*(Ts) strain to the non-permissive temperature (Fig. 2) strongly suggests that SPOR-independent localization of GFP-$FtsN_{Cyto\text{-}TM}$ is mediated by its interaction with FtsA. This conclusion is further supported by the efficient recruitment of GFP-$FtsN_{Cyto\text{-}TM}$ to poles by DivIVA-FtsA and DivIVA-FtsA-E124A (Fig. 4) as well as previously published evidence that FtsA and FtsN interact directly (Busiek et al., 2012). FtsA-dependent localization of FtsN may also explain why FtsN fails to localize to midcell in the absence of FtsA, despite the recruitment of all other essential cell division proteins by a ZapA-FtsQ fusion (Goehring et al., 2005).

The involvement of FtsA in the localization of FtsN also provides a potential explanation for the ability of FtsN to suppress the *ftsA12*(Ts) strain at 37°C (but not at 42°C) when present in a multicopy pBR322 derivative plasmid (Dai et al., 1993). Overproduction of FtsN from the plasmid might partially overcome the need for SPOR-independent localization of FtsN, similar to how overproduction of $VirB10_{Cyto}N_{TM\text{-}Peri}$ is capable of complementing the lack of wild-type FtsN (Fig. 7A, 7C, S4). Overproduction of FtsN or $VirB10_{Cyto}N_{TM\text{-}Peri}$ enriches these proteins in the membrane and likely increases the probability that these proteins will interact with other divisome components. Although we believe that multicopy expression of *ftsN* may bypass the need for FtsA-mediated localization, we do not yet understand how the cytoplasmic and transmembrane domains of FtsN can partially suppress the loss of *ftsK* or *ftsQ* (Geissler and Margolin, 2005, Goehring et al., 2007).

The disparate enrichment of GFP-$FtsN_{\Delta SPOR}$ at non-constricting sites and GFP-$VirB10_{Cyto}N_{TM\text{-}Peri}$ at constricting sites initially suggested to us that SPOR-independent localization of FtsN precedes SPOR-dependent localization of FtsN (Table 3). We confirmed this timing by observing cells that co-produced GFP-tagged $FtsN_{Cyto\text{-}TM}$ and ^{TT}mCherry-tagged $FtsN_{SPOR}$ (Fig. 6). Intriguingly, while ^{TT}mCherry-$FtsN_{SPOR}$ seemed to persist at deep constrictions, GFP-$FtsN_{Cyto\text{-}TM}$ appeared to abandon these sites for nascent division sites (as shown by the loss of GFP-$FtsN_{Cyto\text{-}TM}$ fluorescence at deep constrictions in Fig. 6). This observation suggests that whereas the amino-terminus of FtsN facilitates initial localization of FtsN, this interaction may weaken despite the continuous presence of FtsA at the septum until later stages of cytokinesis. This may be because at later stages, $FtsN_{Cyto\text{-}TM}$ now faces increasing competition with other proteins for its binding site within subdomain 1c of FtsA, including potentially another molecule of FtsA (Pichoff *et al.*, 2012). Another possibility is that FtsA itself begins to leave the divisome prior to septum completion, although a very recent study suggests that FtsA persists until septum closure (Soderstrom *et al.*). In any case, in this model, the main responsibility of maintaining FtsN at the growing septum until completion would then fall to the SPOR domain. The anchoring of FtsN to old division sites by the SPOR domain would prevent premature abandonment by

FtsN as FtsA redeploys to newly assembled Z-rings. This built-in regulation of FtsN localization is likely an important feature of FtsN, as substitution or deletion of either localization determinant reduced cell division and viability (Fig. 7a, 7c, and S4).

While two of our previous publications have explored if and how FtsA and FtsN interact (Corbin et al., 2004, Busiek et al., 2012), this study addresses the more interesting question of why these early and late proteins contact one another. At least one physiological role of FtsA-FtsN interaction is efficient recruitment of FtsN to the divisome, although additional functions of this interaction may also be uncovered. One interesting possibility is that once recruited, FtsN may transduce a signal to FtsA that triggers initiation of Z-ring constriction, but further studies will be needed to address this prospect (Lutkenhaus, 2009, Busiek et al., 2012, Corbin et al., 2004). We also speculate that the role of other early-late cell division protein interactions (Corbin et al., 2004, Karimova et al., 2005) may be to facilitate more robust recruitment of these proteins to the divisome and/or to fine-tune the timing of their localization. This study provides the first evidence for a physiological role of FtsA-FtsN interaction under physiological conditions.

EXPERIMENTAL PROCEDURES

Strains, growth media, and microscopy

Escherichia coli strains and plasmids used in this study are listed in Table 1. All cultures were grown in Luria-Bertani (LB) medium at 37°C, unless otherwise indicated. LB medium was supplemented with ampicillin (Fisher Scientific; 50 μg ml^{-1}), kanamycin (Sigma-Aldrich; 50 μg ml^{-1}), chloramphenicol (Acros Organics; 10 μg ml^{-1}), and glucose (Sigma-Aldrich; 1%) as needed. Gene expression from the *trc* promoter in pDSW207 and pDSW210 vectors was induced with isopropyl-ß-D-galactopyranoside (IPTG) at a final concentration of 10–100 μM. The *araBAD* promoter in pBAD33 vectors was induced at a final concentration of 0.2% L-arabinose and the *nahR* promoter in pKG116 vectors was induced with 1.0 μM sodium salicylate. Wild type strain WM1074 (TX3772, a *lac*- derivative of MG1655) was used for expression from all plasmids except where noted. To inhibit FtsI activity, cultures were treated with cephalexin (Sigma-Aldrich) at a final concentration of 200 μg mL^{-1} for 30 or 60 minutes. The *ftsN* depletion strain WM4028 was created by transducing strain WM1074 carrying pWM2964 (a temperature sensitive depletion plasmid encoding *ftsN*) with P1 phage carrying Δ*ftsN::kan*, selecting for Kan^R colonies, and screening for colonies that could grow at 30°C but not at 42°C. Similarly, strain WM3302 was constructed by transducing strain WM2935 (W3110 Tn*10 ftsA-E124A*) with Δ*ftsN::kan* P1 lysate and selecting for Kan^R survivors.

Strains were observed using an Olympus BX60 microscope and UPlanSApo 100X oil immersion objective. Differential interference contrast (DIC) and fluorescence images were captured on a Hamamatsu Digital Camera (Model C8484) using HCImageLive (Hamamatsu) software. Membranes were stained as needed to assist visualization by incubating 1 mL cultures with 0.5 μg mL^{-1} FM4–64 stain for 15 minutes at room temperature.

Plasmid constructions

Plasmids and primer sequences are listed in Table 1 and Table S1, respectively. Following the manufacturer's guidelines, DNA was amplified using KAPA HiFi DNA polymerase from VWR (Radnor, PA) and primers from Sigma-Aldrich (St. Louis, MO) and Integrated DNA Technologies (IDT, Coralville, IA). Restriction and T4 DNA ligase enzymes were purchased from New England BioLabs, Inc. (NEB; Beverly, MA) and DNA cleanup kits were obtained from Promega (Madison, WI). Clones were sequenced by Genewiz (South Plainfield, NJ).

The polar recruitment assay vector pWM4637 (pBAD33-*divIVA-ftsA-E124A*) was constructed by amplifying the *ftsA-E124A* gene from template plasmid pWM2702 (pRR48-*flag-ftsA-E124A*) with primers 2051 and 2052. The PCR product and recipient vector pBAD33-*divIVA* were then digested with *Xba*I and *Pst*I and ligated.

To create pWM4740 (pKG116-^{TT}*mCherry-ftsN*$_{SPOR}$), ^{TT}*mCherry-ftsN*$_{SPOR}$ was amplified from template pWM4682 (pDSW208-^{TT}*mCherry-ftsN*$_{SPOR}$) using primers 2063 and 2059. The insert was then cloned into vector pKG116 as an *Nsi*I-*Xba*I fragment. To construct the original template plasmid pWM4682, the signal sequence of *torA* was amplified with primers 2056 and 2055 from pWM1487 (pBAD24-^{TT}*gfp*) and the *mCherry* sequence was amplified with primers 2054 and 2057 from pWM4367 (pDSW208-*ftsZ*$_{1–176}$-*mCherry-ftsZ*$_{177–383}$). The *torA* signal sequence and *mCherry* were then fused using combinatorial PCR (primers 2056 and 2057) to create a ^{TT}*mCherry* fragment that was cloned into pDSW208 using *Eco*RI and *Bam*HI restriction sites. The SPOR domain of *ftsN* was then amplified from template pWM1152 (pDSW207-*ftsN*) with primers 2058 and 2059 and cloned into pDSW208-^{TT}*mCherry* as a *Bam*HI-*Xba*I fragment.

All pWM2784 (pDSW210-*flag*) derivatives engineered for this study were cloned as *Xba*I-*Pst*I fragments. To create plasmid pWM3157 (pDSW210-*flag-ftsN*), the *ftsN* insert was amplified with primers 1115 and 1116. Plasmid pWM4582 (pDSW210-*flag-virB10*$_{Cyto}$*N*$_{TM-Peri}$) was created by amplifying the sequences encoding the cytoplasmic domain of *virB10* with primers 1809 and 1804 and the transmembrane and periplasmic domains of *ftsN* with primers 1803 and 1116. The PCR products were then joined in a combinatorial PCR reaction with primers 1809 and 1116. To create plasmid pWM4612 (pDSW210-*flag-virB10*$_{Cyto}$*N*$_{TM-Peri\Delta SPOR}$), the *virB10*$_{Cyto}$*N*$_{TM-Peri\Delta SPOR}$ sequence was amplified from template pWM4582 (pDSW210-*flag-virB10*$_{Cyto}$*N*$_{TM-Peri}$) using forward primer 1809 and reverse primer 2049 to omit the SPOR sequence from the PCR product. The pDSW210-*flag-ftsN*$_{\Delta SPOR}$ plasmid pWM4613 was constructed by amplifying *ftsN*$_{\Delta SPOR}$ from template pWM3157 (pDSW210-*flag-ftsN*) using primers 1115 and 2049 to also omit the SPOR sequence.

Insertion of DNA sequences into the multiple cloning site of vector pDSW207 fuses GFP to the amino terminus of encoded proteins. The GFP-FtsZ fusion produced from pWM3775 (pDSW207-*gfp-ftsZ*) was created by subcloning *ftsZ* from pDSW209-*gfp-ftsZ* (pWM3439) into vector pDSW207 using *Sac*I and *Hind*III restriction sites. All other pDSW207 plasmids were constructed using *Eco*RI and *Hind*III sites and all forward primers included a sequence to create an Asn-Asn-Asn linker between GFP and the protein of interest. pWM4528

(pDSW207-*gfp-ftsN*$_{Cyto\text{-}TM}$) was created by amplifying the cytoplasmic and transmembrane regions of *ftsN* from template pWM1152 (pDSW207-*gfp-ftsN*) with primers 112 and 2003. To construct pWM4610 (pDSW207-*gfp-virB10*$_{Cyto}$*N*$_{TM}$), *virB10*$_{Cyto}$*N*$_{TM}$ was amplified from template pWM4582 (pDSW210-*flag-virB10*$_{Cyto}$*N*$_{TM\text{-}Peri}$) with primers 2048 and 2003. pWM4611 (pDSW207-*gfp-ftsN*$_{Cyto}$*virB10*$_{TM}$) was cloned by amplifying the cytoplasmic and transmembrane domains of pWM4432 (pKT25-*flag-ftsN*$_{Cyto}$*virB10*$_{TM}$*phoA*) using primers 112 and 2047. For pWM4696 (pDSW207-*gfp-virB10*$_{Cyto}$*N*$_{TM\text{-}Peri}$), the *virB10*$_{Cyto}$*N*$_{TM\text{-}Peri}$ sequence was amplified from pWM4582 (pDSW210-*flag-virB10*$_{Cyto}$*N*$_{TM\text{-}Peri}$) using primers 2048 and 111. To create pDSW207-*gfp-ftsN*$_{\Delta SPOR}$ (pWM4693), *ftsN*$_{\Delta SPOR}$ was amplified from pWM4613 (pDSW210-*flag-ftsN*) using primers 112 and 2060. Finally, pWM4694 (pDSW207-*gfp-virB10*$_{Cyto}$*N*$_{TM\text{-}Peri\Delta SPOR}$) was cloned by amplifying *virB10*$_{Cyto}$*N*$_{TM\text{-}Peri\Delta SPOR}$ from pWM4612 (210-*flag-virB10*$_{Cyto}$*N*$_{TM\text{-}Peri\Delta SPOR}$) using primers 2048 and 2060.

Temperature-shift experiments with ftsA12(Ts)

Cultures of *ftsA12*(Ts) strain WM1115 expressing *gfp* (pWM1088), *gfp-ftsN*$_{Cyto\text{-}TM}$ (pWM4528), *gfp-ftsN* (pWM1152), *gfp-ftsZ* (pWM3775), or ^{TT}*mCherry-ftsN*$_{SPOR}$ (pWM4740) were grown at 30°C to an optical density at 600nm (OD_{600}) of 0.3–0.4 prior to temperature shift. Strains expressing *gfp* fusions from vector pDSW207 remained uninduced throughout the experiment, whereas the strain expressing ^{TT}*mCherry-ftsN*$_{SPOR}$ from pKG116 was grown in the presence of 1 μM sodium salicylate. Cultures were shifted to 42°C for 5 minutes. DIC and fluorescence images were obtained at each time point.

Polar recruitment assay

Cultures of strains carrying the pBAD33-*divIVA-ftsA* (pWM1806) or pBAD33-*divIVA-ftsA-E124A* (pWM4637) vector and pDSW207 plasmids expressing *gfp* (pWM1088), *gfp-ftsN*$_{Cyto\text{-}TM}$ (pWM4528), or *gfp-ftsN* (pWM1152) were grown and induced as described previously (Corbin et al., 2004). Briefly, cultures were grown at 30°C to a low OD_{600} (~0.1) and induced for 1.5–2 hours with 40 μM IPTG only (inducing expression from pDSW207 plasmids) or 40 μM IPTG plus 0.2% arabinose (inducing expression from pDSW207 and pBAD33 plasmids).

ΔftsN::kan transductions and depletion experiments

To obtain transductants harboring the Δ*ftsN::kan* allele, wild-type cells containing plasmid pWM2784 (pDSW210-*flag*), pWM4612 (pDSW210-*flag-virB10*$_{Cyto}$*ftsN*$_{TM\text{-}Peri\Delta SPOR}$), pWM4582 (pDSW210-*flag-virB10*$_{Cyto}$*ftsN*$_{TM\text{-}Peri}$), pWM4613 (pDSW210-*flag-ftsN*$_{\Delta SPOR}$), or pWM3643 (pDSW210-*flag-ftsN*) were grown to low OD_{600} (~0.2) and transduced with a P1 phage lysate derived from Δ*ftsN::kan* strain WM3303, which also carries the *ftsA-E124A* allele to permit survival in the absence of FtsN. Following a one hour outgrowth in media containing 10 mM sodium citrate, cells were plated onto media containing kanamycin and ampicillin to select for the plasmids and Δ*ftsN::kan*, and with 0, 10, or 100 μM IPTG to induce expression from the pDSW210 vector. Survivors were picked from the plates containing 100 μM IPTG, grown at 37°C to an OD_{600} ≤0.5 in selective medium containing 100 μM IPTG, and visualized by DIC microscopy. Cells were then washed three times to

remove IPTG and grown in the absence of inducer to decrease expression from the pDSW210 vector. Cultures were back-diluted as needed to maintain a low-mid OD_{600}. Cells were visualized every hour following exposure to depletion conditions for a total of 4 hours.

To obtain samples for immunoblot analysis, plasmids pWM4612 (pDSW210-*flag-virB10*$_{Cyto}$*ftsN*$_{TM\text{-}Peri\Delta SPOR}$), pWM4582 (pDSW210-*flag-virB10*$_{Cyto}$*ftsN*$_{TM\text{-}Peri}$), pWM4613 (pDSW210-*flag-ftsN*$_{\Delta SPOR}$), and pWM3643 (pDSW210-*flag-ftsN*) were transformed into *ftsN* depletion strain WM4028, grown at the permissive temperature of 30°C to low-mid OD_{600} in the absence of inducer, and shifted to 42°C in the presence of 10 or 100 μM IPTG for 4 hours. Cultures were continually back-diluted throughout the experiment to remain in logarithmic phase. Cultures were then normalized based on OD_{600} and boiled in sodium dodecyl sulfate (SDS) dye for 10 minutes prior to storage at −20°C.

Immunoblot analysis

Samples from the FtsN depletion strain were collected as described above and separated by SDS-PAGE, using equal volumes of normalized samples per lane. Using a wet apparatus, FLAG-tagged proteins were transferred onto a nitrocellulose membrane and stained with Swift membrane stain (G-Biosciences; St. Louis, MO) to show that similar levels of proteins in all lanes were loaded and transferred. The membrane was immunoblotted with mouse monoclonal anti-FLAG antibody (1:5,000) and goat anti-mouse secondary antibody conjugated to horseradish peroxidase (HRP; 1:10,000). HRP was detected using Western Lightning ECL Pro (PerkinElmer, Inc., Waltham, MA) and quantified using Image Studio Software (LI-COR; Lincoln, NE).

Supplementary Material

Refer to Web version on PubMed Central for supplementary material.

Acknowledgments

We thank past and present Margolin lab members for insightful comments and suggestions. We also thank Jennifer Herricks for sharing affinity purified α-FtsA antibody.

This work was supported by NIGMS grant 61074.

REFERENCES

Aarsman ME, Piette A, Fraipont C, Vinkenvleugel TM, Nguyen-Disteche M, den Blaauwen T. Maturation of the *Escherichia coli* divisome occurs in two steps. Mol Microbiol. 2005; 55:1631–1645. [PubMed: 15752189]

Addinall SG, Cao C, Lutkenhaus J. FtsN, a late recruit to the septum in *Escherichia coli*. Mol Microbiol. 1997; 25:303–309. [PubMed: 9282742]

Alexeeva S, Gadella TW Jr. Verheul J, Verhoeven GS, den Blaauwen T. Direct interactions of early and late assembling division proteins in *Escherichia coli* cells resolved by FRET. Mol Microbiol. 2010; 77:384–398. [PubMed: 20497333]

Arends SJ, Williams K, Scott RJ, Rolong S, Popham DL, Weiss DS. Discovery and characterization of three new *Escherichia coli* septal ring proteins that contain a SPOR domain: DamX, DedD, and RlpA. J Bacteriol. 2010; 192:242–255. [PubMed: 19880599]

Bernard CS, Sadasivam M, Shiomi D, Margolin W. An altered FtsA can compensate for the loss of essential cell division protein FtsN in *Escherichia coli*. Mol Microbiol. 2007; 64:1289–1305. [PubMed: 17542921]

Bi E, Lutkenhaus J. FtsZ ring structure associated with division in *Escherichia coli*. Nature. 1991; 354:161–164. [PubMed: 1944597]

Busiek KK, Eraso JM, Wang Y, Margolin W. The early divisome protein FtsA interacts directly through its 1c subdomain with the cytoplasmic domain of the late divisome protein FtsN. J Bacteriol. 2012; 194:1989–2000. [PubMed: 22328664]

Chung HS, Yao Z, Goehring NW, Kishony R, Beckwith J, Kahne D. Rapid beta-lactam-induced lysis requires successful assembly of the cell division machinery. Proc Natl Acad Sci USA. 2009; 106:21872–21877. [PubMed: 19995973]

Corbin BD, Geissler B, Sadasivam M, Margolin W. Z-ring-independent interaction between a subdomain of FtsA and late septation proteins as revealed by a polar recruitment assay. J Bacteriol. 2004; 186:7736–7744. [PubMed: 15516588]

Dai K, Xu Y, Lutkenhaus J. Cloning and characterization of *ftsN* an essential cell division gene in *Escherichia coli* isolated as a multicopy suppressor of *ftsA12*(Ts). J Bacteriol. 1993; 175:3790–3797. [PubMed: 8509333]

Dai K, Xu Y, Lutkenhaus J. Topological characterization of the essential *Escherichia coli* cell division protein FtsN. J Bacteriol. 1996; 178:1328–1334. [PubMed: 8631709]

Ding Z, Zhao Z, Jakubowski SJ, Krishnamohan A, Margolin W, Christie PJ. A novel cytology-based, two-hybrid screen for bacteria applied to protein-protein interaction studies of a Type IV secretion system. J Bacteriol. 2002; 184:5572–5582. [PubMed: 12270814]

Edwards DH, Thomaides HB, Errington J. Promiscuous targeting of *Bacillus subtilis* cell division protein DivIVA to division sites in *Escherichia coli* and fission yeast. EMBO J. 2000; 19:2719–2727. [PubMed: 10835369]

Erickson HP. FtsZ, a tubulin homologue in prokaryote division. Trends Cell Biol. 1997; 7:362–367. [PubMed: 17708981]

Garza I, Christie PJ. A putative transmembrane leucine zipper of *Agrobacterium* VirB10 is essential for T-pilus biogenesis but not type IV secretion. J Bacteriol. 2013; 195:3022–3034. [PubMed: 23625845]

Geissler B, Elraheb D, Margolin W. A gain of function mutation in *ftsA* bypasses the requirement for the essential cell division gene *zipA* in *Escherichia coli*. Proc Natl Acad Sci USA. 2003; 100:4197–4202. [PubMed: 12634424]

Geissler B, Margolin W. Evidence for functional overlap among multiple bacterial cell division proteins: compensating for the loss of FtsK. Mol Microbiol. 2005; 58:596–612. [PubMed: 16194242]

Gerding MA, Liu B, Bendezu FO, Hale CA, Bernhardt TG, de Boer PA. Self-enhanced accumulation of FtsN at division sites and roles for other proteins with a SPOR domain (DamX, DedD, and RlpA) in *Escherichia coli* cell constriction. J Bacteriol. 2009; 191:7383–7401. [PubMed: 19684127]

Goehring NW, Beckwith J. Diverse paths to midcell: assembly of the bacterial cell division machinery. Curr Biol. 2005; 15:514–526.

Goehring NW, Gueiros-Filho F, Beckwith J. Premature targeting of a cell division protein to midcell allows dissection of divisome assembly in *Escherichia coli*. Genes Dev. 2005; 19:127–137. [PubMed: 15630023]

Goehring NW, Petrovska I, Boyd D, Beckwith J. Mutants, suppressors, and wrinkled colonies: Mutant alleles of the cell division gene ftsQ point to functional domains in FtsQ and a role for domain 1C of FtsA in divisome assembly. J Bacteriol. 2007; 189:633–645. [PubMed: 16980443]

Guzman LM, Belin D, Carson MJ, Beckwith J. Tight regulation, modulation, and high-level expression by vectors containing the arabinose PBAD promoter. J Bacteriol. 1995; 177:4121–4130. [PubMed: 7608087]

Guzman LM, Weiss DS, Beckwith J. Domain-swapping analysis of FtsI, FtsL, and FtsQ, bitopic membrane proteins essential for cell division in *Escherichia coli*. J Bacteriol. 1997; 179:5094–5103. [PubMed: 9260951]

Karimova G, Dautin N, Ladant D. Interaction network among *Escherichia coli* membrane proteins involved in cell division as revealed by bacterial two-hybrid analysis. J Bacteriol. 2005; 187:2233–2243. [PubMed: 15774864]

Lutkenhaus J. FtsN--trigger for septation. J Bacteriol. 2009; 191:7381–7382. [PubMed: 19854895]

Ma X, Ehrhardt DW, Margolin W. Colocalization of cell division proteins FtsZ and FtsA to cytoskeletal structures in living *Escherichia coli* cells by using green fluorescent protein. Proc Natl Acad Sci USA. 1996; 93:12998–13003. [PubMed: 8917533]

Muller P, Ewers C, Bertsche U, Anstett M, Kallis T, Breukink E, Fraipont C, Terrak M, Nguyen-Disteche M, Vollmer W. The essential cell division protein FtsN interacts with the murein (peptidoglycan) synthase PBP1B in *Escherichia coli*. J Biol Chem. 2007; 282:36394–36402. [PubMed: 17938168]

Peters NT, Dinh T, Bernhardt TG. A fail-safe mechanism in the septal ring assembly pathway generated by the sequential recruitment of cell separation amidases and their activators. J Bacteriol. 2011; 193:4973–4983. [PubMed: 21764913]

Pichoff S, Lutkenhaus J. Unique and overlapping roles for ZipA and FtsA in septal ring assembly in *Escherichia coli*. EMBO J. 2002; 21:685–693. [PubMed: 11847116]

Pichoff S, Lutkenhaus J. Tethering the Z ring to the membrane through a conserved membrane targeting sequence in FtsA. Mol Microbiol. 2005; 55:1722–1734. [PubMed: 15752196]

Pichoff S, Shen B, Sullivan B, Lutkenhaus J. FtsA mutants impaired for self-interaction bypass ZipA suggesting a model in which FtsA's self-interaction competes with its ability to recruit downstream division proteins. Mol Microbiol. 2012; 83:151–167. [PubMed: 22111832]

Raychaudhuri D. ZipA is a MAP-Tau homolog and is essential for structural integrity of the cytokinetic FtsZ ring during bacterial cell division. EMBO J. 1999; 18:2372–2383. [PubMed: 10228152]

Rico AI, Garcia-Ovalle M, Palacios P, Casanova M, Vicente M. Role of *Escherichia coli* FtsN protein in the assembly and stability of the cell division ring. Mol Microbiol. 2010; 76:760–771. [PubMed: 20345660]

Rico AI, Krupka M, Vicente M. In the beginning, *Escherichia coli* assembled the proto-ring: an initial phase of division. J Biol Chem. 2013; 288:20830–20836. [PubMed: 23740256]

Shiomi D, Margolin W. Dimerization or oligomerization of the actin-like FtsA protein enhances the integrity of the cytokinetic Z ring. Mol Microbiol. 2007; 66:1396–1415. [PubMed: 17986188]

Shiomi D, Margolin W. Compensation for the loss of the conserved membrane targeting sequence of FtsA provides new insights into its function. Mol Microbiol. 2008; 67:558–569. [PubMed: 18186792]

Söderström B, Skoog K, Blom H, Weiss DS, von Heijne G, Daley DO. Disassembly of the divisome in *Escherichia coli*: Evidence that FtsZ dissociates before compartmentalization. Mol Microbiol. 2014; 92:1–9. [PubMed: 24506818]

Thomas JD, Daniel RA, Errington J, Robinson C. Export of active green fluorescent protein to the periplasm by the twin-arginine translocase (Tat) pathway in *Escherichia coli*. Mol Microbiol. 2001; 39:47–53. [PubMed: 11123687]

Ursinus A, van den Ent F, Brechtel S, de Pedro M, Holtje JV, Löwe J, Vollmer W. Murein (peptidoglycan) binding property of the essential cell division protein FtsN from *Escherichia coli*. J Bacteriol. 2004; 186:6728–6737. [PubMed: 15466024]

Vicente M, Rico AI. The order of the ring: assembly of *Escherichia coli* cell division components. Mol Microbiol. 2006; 61:5–8. [PubMed: 16824090]

Weiss DS, Chen JC, Ghigo JM, Boyd D, Beckwith J. Localization of FtsI (PBP3) to the septal ring requires its membrane anchor, the Z ring, FtsA, FtsQ, and FtsL. J Bacteriol. 1999; 181:508–520. [PubMed: 9882665]

Wissel MC, Wendt JL, Mitchell CJ, Weiss DS. The transmembrane helix of the *Escherichia coli* division protein FtsI localizes to the septal ring. J Bacteriol. 2005; 187:320–328. [PubMed: 15601716]

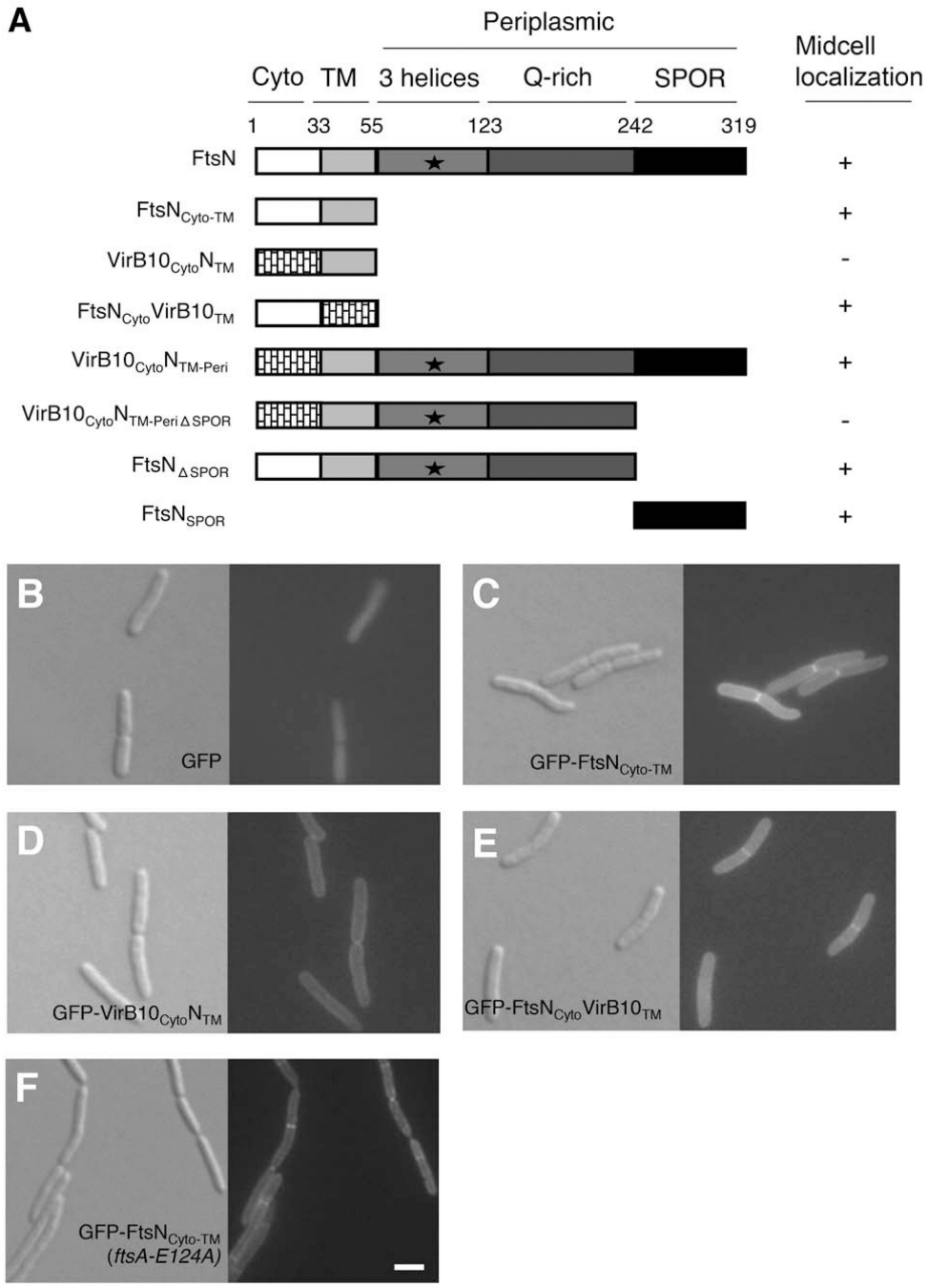

FIG. 1. The cytoplasmic domain of FtsN contributes to midcell localization independently of native FtsN

(A) Domain organization of FtsN and engineered constructs used in this study. Midcell localization of each GFP-tagged construct in a wild-type strain is indicated by a (+) symbol; diffuse or peripheral membrane localization is noted by a (−) symbol. The essential region of FtsN (aa71–105; Gerding *et al.* 2009) is represented by a black star. (B–F) DIC (left) and fluorescence (right) images of cells grown to low OD_{600} at 37°C in the absence of IPTG. Cells shown in panels B–E are wild-type WM1074 harboring plasmids pWM1088 (pDSW207-*gfp*) (B), pWM4528 (pDSW207-*gfp-ftsN*$_{Cyto-TM}$) (C), pWM4610 (pDSW207-

gfp-virB10$_{Cyto}$*N*$_{TM}$) (D), or pWM4611 (pDSW207-*gfp-ftsN*$_{Cyto}$*virB10*$_{TM}$) (E). Cells shown in (F) lack the native *ftsN* allele but harbor a single chromosomal copy of *ftsA-E124A* (WM3303 background) as well as plasmid pWM4528 (pDSW207-*gfp-ftsN*$_{Cyto\text{-}TM}$). Scale bar = 4 μm.

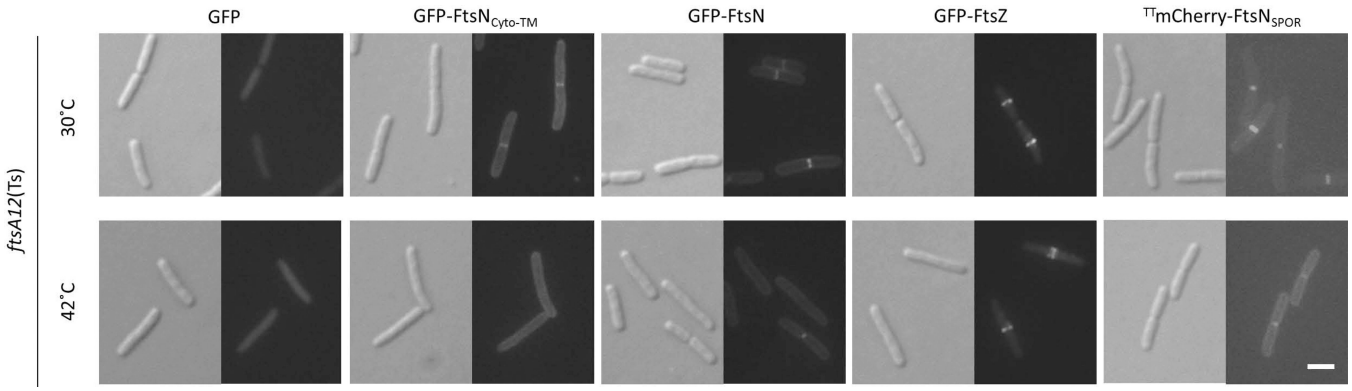

FIG. 2. Localization of GFP-FtsN$_{Cyto-TM}$ to midcell is dependent on FtsA

DIC (left) and fluorescence (right) images of *ftsA12*(Ts) strains harboring plasmids pWM1088 (pDSW207-*gfp*), pWM4528 (pDSW207-*gfp-ftsN*$_{Cyto-TM}$), pWM1152 (pDSW207-*gfp-ftsN*), pWM3775 (pDSW207-*gfp-ftsZ*), or pWM4740 (pKG116-^{TT}*mCherry-ftsN*$_{SPOR}$). Cells were grown to low OD_{600} without IPTG (strains containing pDSW207 derivatives) or with 1 μM sodium salicylate (strain containing pKG116 derivative) at 30°C then shifted to 42°C for 5 minutes. Scale bar = 4 μm.

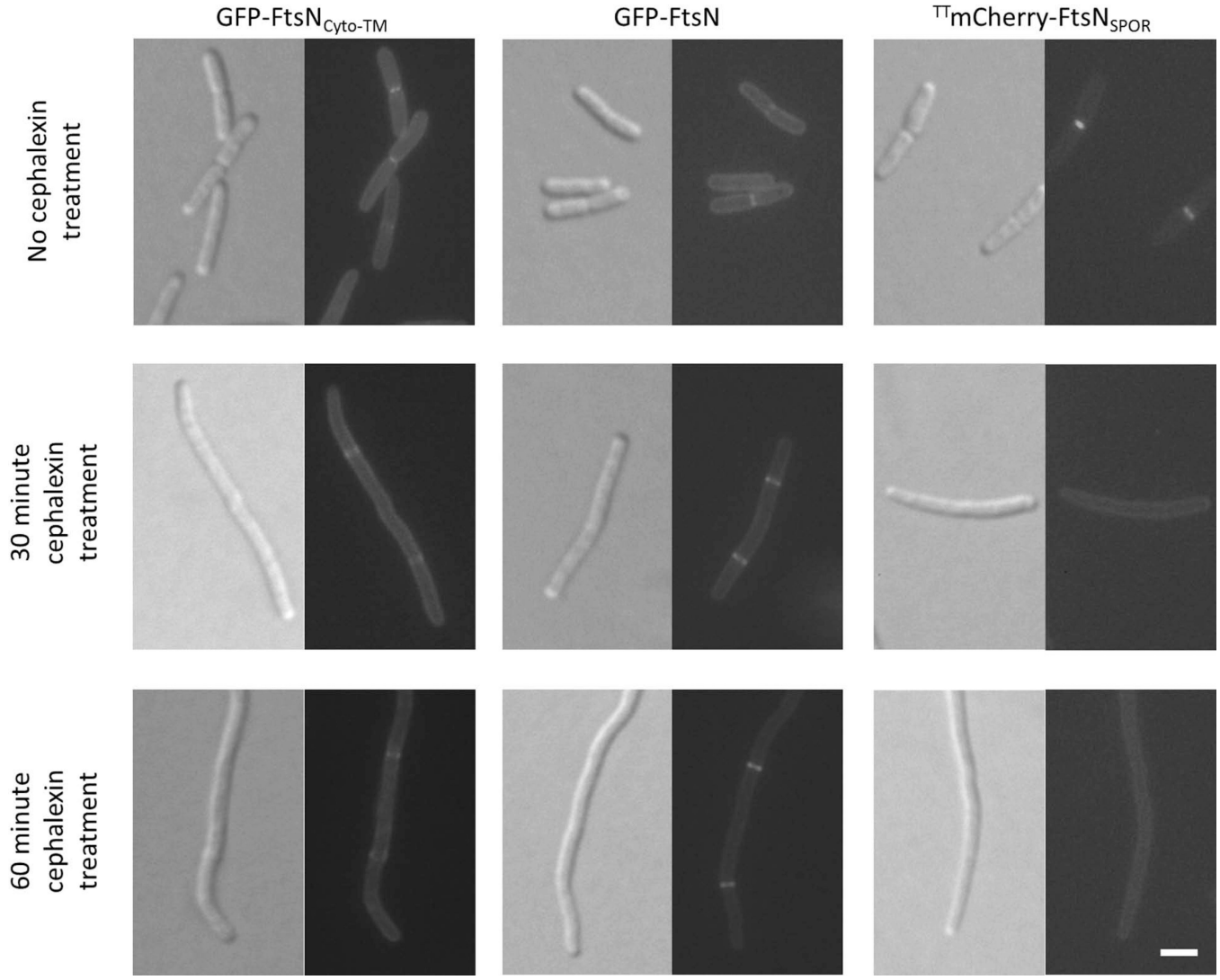

FIG. 3. Localization of GFP-tagged FtsN$_{Cyto-TM}$ and FtsN is not dependent on FtsI activity

DIC (left) and fluorescence (right) images of wild-type (WM1074) strains harboring plasmids pWM4528 (pDSW207-*gfp-ftsN*$_{Cyto-TM}$), pWM1152 (pDSW207-*gfp-ftsN*), or pWM4740 (pKG116-^{TT}*mCherry-ftsN*$_{SPOR}$). Cells were grown to low OD_{600} without IPTG (strains containing pDSW207 derivatives) or with 1 μM sodium salicylate (strain containing pKG116 derivative) at 37°C. Cultures were back-diluted 1:1 and imaged at 30 minutes and 60 minutes after addition of cephalexin to inhibit FtsI activity. Cultures were also back-diluted after the 30-minute time point to maintain a low OD_{600}. Scale bar = 4 μm.

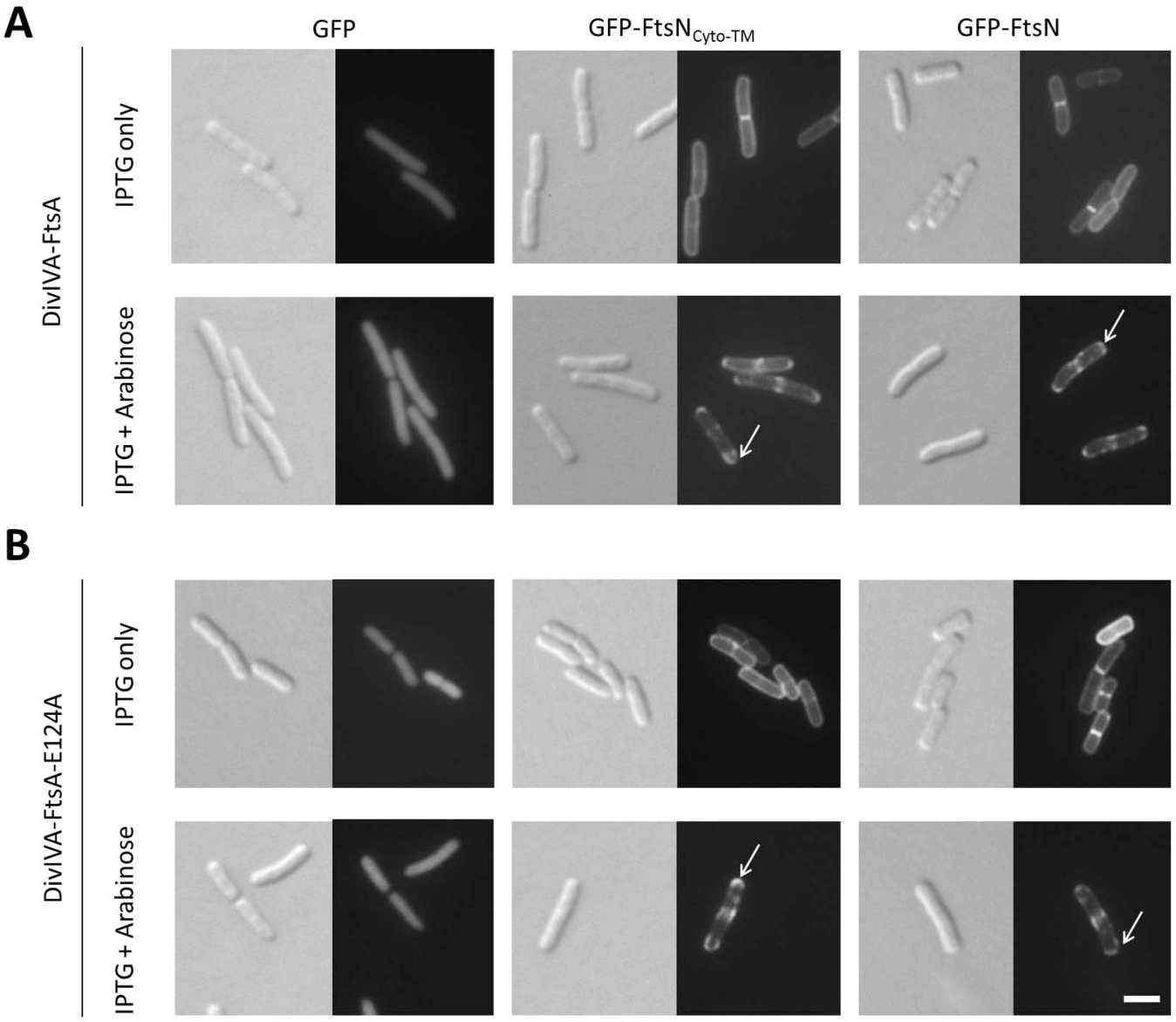

FIG. 4. DivIVA-FtsA and DivIVA-FtsA-E124A recruit GFP-FtsN$_{Cyto-TM}$ to cell poles

Images are of wild-type cells containing pWM1088 (pDSW207-*gfp*), pWM4528 (pDSW207-*gfp-ftsN$_{Cyto-TM}$*), or pWM1152 (pDSW207-*gfp-ftsN*) plus either pWM1806 (pBAD33-*divIVA-ftsA*) (A) or pWM4637 (pBAD33-*divIVA-ftsA-E124A*) (B). Cells were grown to low OD_{600} at 30°C and then induced for two hours with either 40 μM IPTG only (to induce expression from pDSW207 plasmids) or 40 μM IPTG plus 0.2% arabinose (to induce expression from both plasmids). White arrows indicate examples of polar localization of GFP-tagged constructs. Scale bar = 4 μm.

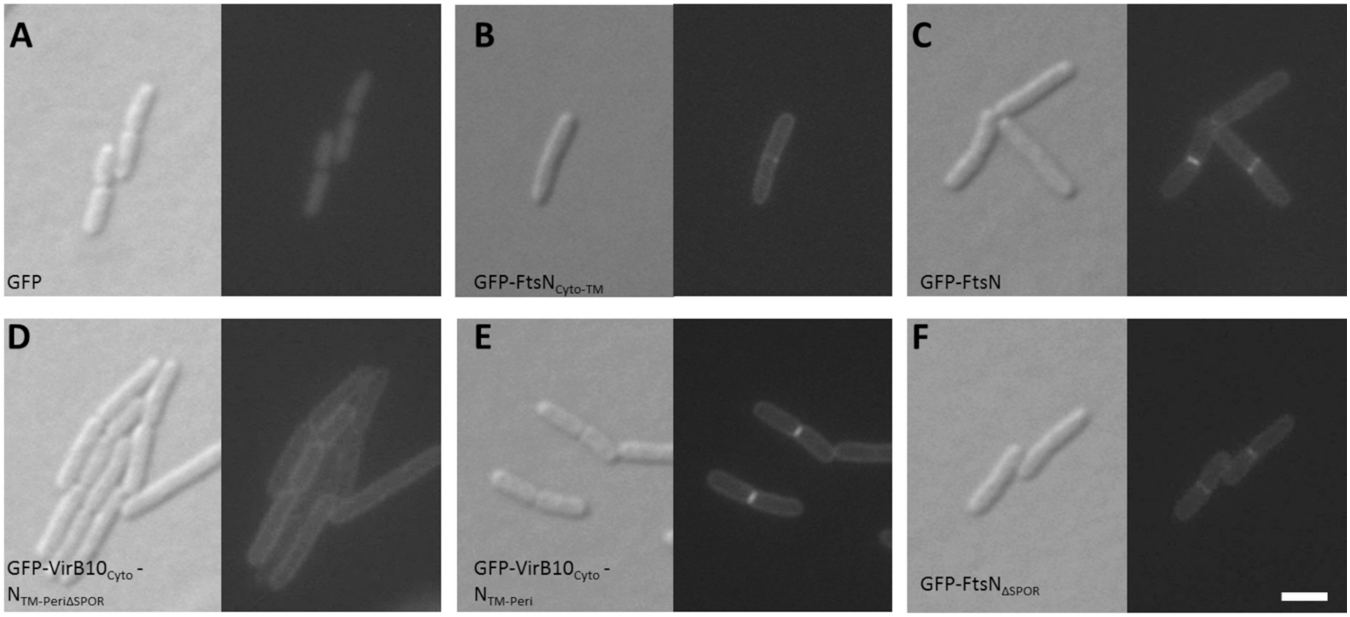

FIG. 5. Removal of both cytoplasmic and SPOR domains of FtsN abolishes midcell localization

DIC (left) and fluorescence (right) images of wild-type strains containing plasmid pWM1088 (pDSW207-*gfp*) (A), pWM4528 (pDSW207-*gfp-ftsN*$_{Cyto-TM}$) (B), pWM1152 (pDSW207-*gfp-ftsN*) (C), pWM4694 (pDSW207-*gfp-virB10*$_{Cyto}$*N*$_{TM-PeriΔSPOR}$) (D), pWM4696 (pDSW207-*gfp-virB10*$_{Cyto}$*N*$_{TM-Peri}$) (E), or pWM4693 (pDSW207-*gfp-ftsN*$_{ΔSPOR}$) (F). Cultures were grown to low OD_{600} at 30°C without inducer before visualization. Scale bar = 4 μm.

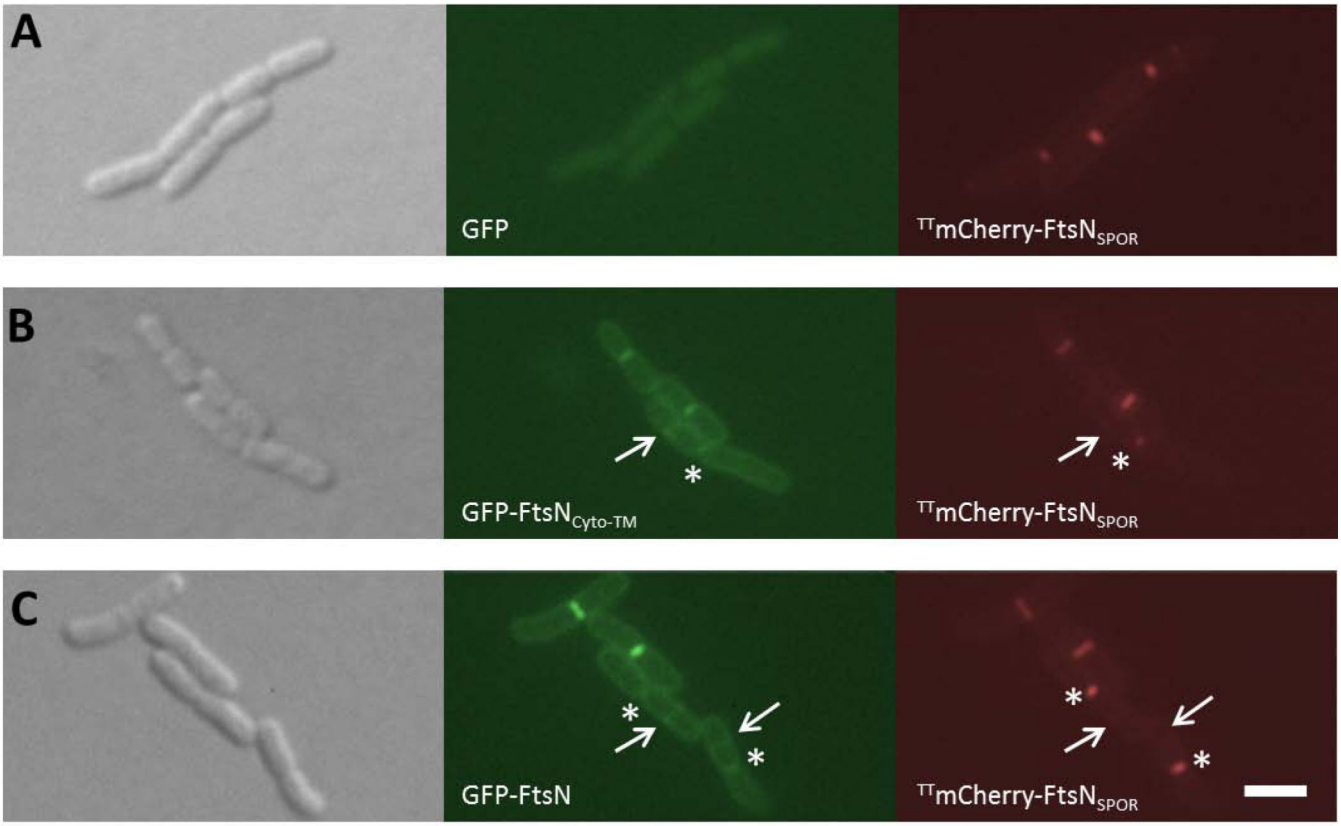

Fig. 6. GFP-FtsN$_{Cyto\text{-}TM}$ localizes to division sites prior to ^{TT}mCherry-FtsN$_{SPOR}$

DIC (left), GFP (middle), and mCherry (right) filter sets were used to capture images of cells grown to low OD_{600} at 30°C in the absence of inducers. All strains were wild-type background and contained plasmid pWM4740 (pKG116-^{TT}*mCherry-ftsN$_{SPOR}$*) plus either plasmid pWM1088 (pDSW207-*gfp*) (A), pWM4528 (pDSW207-*gfp-ftsN$_{Cyto\text{-}TM}$*) (B), or pWM1152 (pDSW207-*gfp-ftsN*) (C). Arrows denote division site localization of GFP-tagged proteins only and asterisks mark localization of ^{TT}mCherry-FtsN$_{SPOR}$ only. Scale bar = 4 μm.

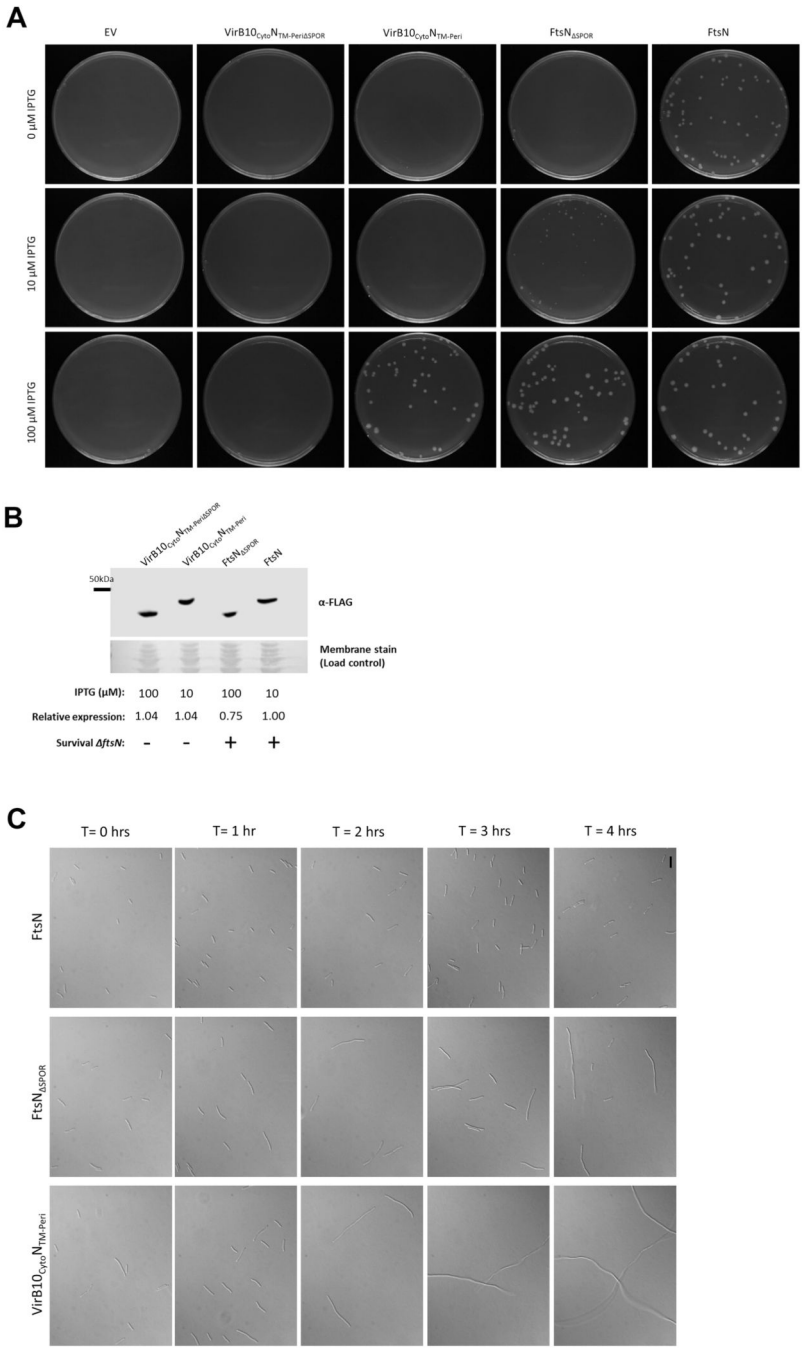

FIG. 7. The cytoplasmic and SPOR domains are both needed for full FtsN function in cell division

(A) Δ*ftsN::kan* P1 transduction of wild-type strains containing pWM2784 (pDSW210-*flag*), pWM4582 (pDSW210-*flag-virB10*$_{Cyto}$*N*$_{TM\text{-}Peri}$), or pWM3157 (pDSW210-*flag-ftsN*). Transductants were plated onto LB medium containing 0, 10, or 100 μM IPTG. (B) α-FLAG Western blot analysis of FLAG-VirB10$_{Cyto}$N$_{TM\text{-}Peri\Delta SPOR}$, FLAG-VirB10$_{Cyto}N_{TM\text{-}Peri}$, FLAG-FtsN$_{\Delta SPOR}$, and FLAG-FtsN produced from *ftsN*(Ts) strain WM4028. Samples were collected after strains were grown without IPTG to low OD_{600} at 30°C and subsequently shifted to 42°C at various levels of IPTG induction for 4 hours. The ability of the FtsN

constructs to survive P1 transduction at the various levels of IPTG induction are represented by (+) and (−) symbols. (C) DIC images of transductants isolated in (A). Cultures were grown in the presence of 100 μM IPTG to low-mid OD_{600} at 37°C and visualized (T = 0 hours). Cells were then washed and grown in the absence of IPTG for four hours (T = 1, 2, 3, and 4 hours) and back-diluted as needed to prevent entry into stationary phase. Scale bar = 12 μm.

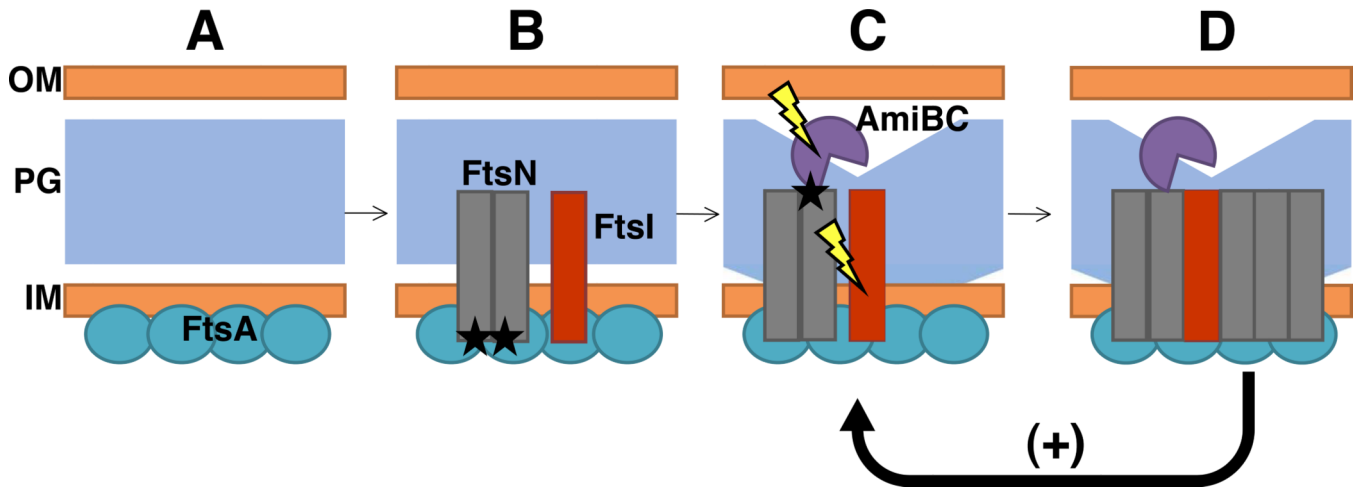

Fig. 8. Proposed role of FtsA-FtsN interactions in cell division

Following midcell localization of FtsA (A), interaction between FtsA and the amino-terminus of FtsN weakly recruits FtsN to midcell in a SPOR-independent manner (B; black asterisks represent recruitment). The small fraction of FtsN localized at midcell recruits amidases AmiB and AmiC and stimulates the peptidoglycan synthesis activity of FtsI. Activities of amidases AmiB and AmiC are stimulated by their cognate activators including FtsN-dependent NlpD (not shown) to degrade peptidoglycan (C; lightning bolt graphic represents stimulation of activity). Peptidoglycan remodeling at midcell exposes denuded glycan strands which, in turn, promote SPOR-dependent localization of FtsN (D). Additional FtsN molecules at the division site stimulate further peptidoglycan remodeling in a positive feedback loop, represented by a “+” symbol. OM=outer membrane, PG=peptidoglycan, IM=inner membrane.

TABLE 1
Strains and plasmids used in this study

Strain or plasmid	Genotype or description	Source or reference
E. coli strains		
WM1074	MG1655 *lacU169* (TX3772)	Laboratory collection
WM1115	TX3772 *leu*::Tn*10 ftsA12*(Ts)	Geissler *et al.* (2003)
WM2935	W3110 (WT strain) *leu*::Tn*10 ftsA-E124A*	Shiomi and Margolin (2008)
WM3302	WM2935 Δ*ftsN::kan*	This study
WM4028	WM1074 Δ*ftsN::kan* pWM2964	This study
Plasmids		
Vectors		
pBAD33	Derivative of pDHB60 with araBAD promoter (Cm^R)	Guzman *et al.* (1995)
pDSW210	P_{trc}-*gfp* pBR322 derivative with weak promoter (Amp^R)	Weiss *et al.* (1999)
pDSW207	P_{trc}-*gfp* pBR322 derivative with strong promoter (Amp^R)	Weiss *et al.* (1999)
pKG116	pACYC184 derivative containing the *nahG* promoter (Cm^R)	J.S. Parkinson
divIVA fusions		
pWM1806	*divIVA-ftsA* in pBAD33	Corbin et al. (2004)
pWM4637	*divIVA-ftsA-E124A* in pBAD33	This study
flag fusions		
pWM2784	*flag* epitope inserted between *Eco*RI and *Sac*I sites of pDSW210	Shiomi and Margolin (2007)
pWM3157	*flag-ftsN* in pDSW210	This study
pWM4582	*flag-virB10*$_{Cyto}$(aa2-32)-*ftsN*$_{TM\text{-}Peri}$(aa29-319) in pDSW210	This study
pWM4612	*flag-virB10*$_{Cyto}$(aa2-32)-*ftsN*$_{TM\text{-}Peri\Delta SPOR}$(aa29-242) in pDSW210	This study
pWM4613	*flag-ftsN*$_{\Delta SPOR}$(aa2-242) in pDSW210	This study
gfp fusions		
pWM1088	*gfp* in pDSW207	Weiss *et al.* (1999)
pWM1152	*gfp-ftsN* in pDSW207	Corbin *et al.* (2004)
pWM3775	*gfp-ftsZ* in pDSW207	This study
pWM4528	*gfp-ftsN*$_{Cyto\text{-}TM}$(aa2-55) in pDSW207	This study
pWM4610	*gfp-virB10*$_{Cyto}$(aa2-32)-*ftsN*$_{TM}$(aa29-55) in pDSW207	This study
pWM4611	*gfp-ftsN*$_{Cyto}$(aa2-33)-*virB10*$_{TM}$(aa33-50) in pDSW207	This study
pWM4693	*gfp-ftsN*$_{\Delta SPOR}$(aa2-242) in pDSW207	This study
pWM4694	*gfp-virB10*$_{Cyto}$(aa2-32)-*ftsN*$_{TM\text{-}Peri\Delta SPOR}$(aa29-242) in pDSW207	This study
pWM4696	*gfp-virB10*$_{Cyto}$(aa2-32)-*ftsN*$_{TM\text{-}Peri}$(aa29-319) in pDSW207	This study
Other plasmids		
pWM4740	^{TT}(*torA* signal sequence)*mCherry-ftsN*$_{SPOR}$(aa241-319) in pKG116	This study
pWM2964	pKD123 (Ts *ftsN* plasmid)	Dai *et al.* (1993)

TABLE 2

Frequency of division site localization of GFP-tagged and ^{TT}mCherry-tagged division proteins in the *ftsA12*(Ts) strain

Cells were grown as described in Figure 2 and imaged live.

Plasmid	Fusion	Total # cells	% Cells with rings at 30°C	% Cells with rings after 5 minutes at 42°C
pWM1088	GFP	233	0	0
pWM4528	GFP-FtsN$_{Cyto-TM}$	211	63	0
pWM1152	GFP-FtsN	595	67	15
pWM3775	GFP-FtsZ	241	94	97
pWM4740	^{TT}mCherry-FtsN$_{SPOR}$	408	88	39

TABLE 3

Frequency of division site localization of GFP-tagged FtsN variants

Cells were grown as described in Figure 4 and imaged live. Visible constriction of cells was determined using DIC images and FM4-64 staining of cell membrane.

Plasmid	Fusion	Total # cells	% Cells with rings	% Cells without rings	% Rings at no constrictions	% Rings at constrictions
pWM1152	GFP-FtsN	130	72	28	57	43
pWM4528	GFP-$FtsN_{Cyto-TM}$	165	56	44	58	42
pWM4693	GFP-$FtsN_{\Delta SPOR}$	139	60	40	62	38
pWM4696	GFP-$VirB10_{Cyto}N_{TM-Peri}$	130	64	36	36	64
pWM4694	GFP-$VirB10_{Cyto}N_{TM-Peri\Delta SPOR}$	142	0	100	NA	NA

TABLE 4

Distinct localization biases of two FtsN domains

Cells were grown as described in Figure 5 and imaged live. Visible constriction of cells was determined using DIC images of each cell.

Plasmids	Fusion	Total # cells	% GFP rings at no constrictions	% GFP rings at constrictions	% mCherry rings at no constrictions	% mCherry rings at constrictions
pWM4528 + pWM4740	GFP-FtsN$_{Cyto-TM}$ + ^{TT}mCherry-FtsN$_{SPOR}$	67	83	16	38	62
pWM1152 + pWM4740	GFP-FtsN + ^{TT}mCherry-FtsN$_{SPOR}$	70	59	41	35	65